Development 140, 2299-2309 (2013) doi:10.1242/dev.094524

Inhibition of Sox2-dependent activation of *Shh* in the ventral diencephalon by Tbx3 is required for formation of the neurohypophysis

Mark-Oliver Trowe[1,*], Li Zhao[2,*], Anna-Carina Weiss[1], Vincent Christoffels[3], Douglas J. Epstein[4,‡] and Andreas Kispert[1,‡]

SUMMARY

Tbx2 and *Tbx3* are two highly related members of the T-box transcription factor gene family that regulate patterning and differentiation of a number of tissue rudiments in the mouse. Both genes are partially co-expressed in the ventral diencephalon and the infundibulum; however, a functional requirement in murine pituitary development has not been reported. Here, we show by genetic lineage tracing that Tbx2$^+$ cells constitute the precursor population of the neurohypophysis. However, *Tbx2* is dispensable for neurohypophysis development as revealed by normal formation of this organ in *Tbx2*-deficient mice. By contrast, loss of *Tbx3* from the ventral diencephalon results in a failure to establish the *Tbx2*$^+$ domain in this region, and a lack of evagination of the infundibulum and formation of the neurohypophysis. Rathke's pouch is severely hypoplastic, exhibits defects in dorsoventral patterning, and degenerates after E12.5. In *Tbx3*-deficient embryos, the ventral diencephalon is hyperproliferative and displays an abnormal cellular architecture, probably resulting from a failure to repress transcription of *Shh*. We further show that Tbx3 and Tbx2 repress *Shh* by sequestering the SRY box-containing transcription factor Sox2 away from a *Shh* forebrain enhancer (*SBE2*), thus preventing its activation. These data suggest that *Tbx3* is required in the ventral diencephalon to establish a *Shh*$^-$ domain to allow formation of the infundibulum.

KEY WORDS: Pituitary gland, Neurohypophysis, Infundibulum, Diencephalon

INTRODUCTION

The hypophysis or pituitary gland is a central regulator of the endocrine system in the control of growth, reproduction and homeostasis. It is composed of two anatomically and functionally distinct units: the neurohypophysis, also referred to as the posterior lobe, and the adenohypophysis, comprising the anterior and intermediate lobes. Adeno- and neurohypophysis derive from different germinal tissues, yet morphogenesis and differentiation of these organs is highly integrated.

In the mouse, morphological changes related to (anterior) pituitary development can first be seen at embryonic day (E) 8.5. At this stage, a subregion of the oral roof ectoderm that lies in close proximity to the ventral neuroectoderm of the forebrain thickens and starts to invaginate shortly afterwards to form Rathke's pouch. Driven by continuous proliferation in its ventral aspect, the pouch continues to grow, and pinches off the oral roof ectoderm to form a closed vesicle by E11.5. Further proliferation of precursor cells within the primitive adenohypophysis and subsequent differentiation leads to the formation of anterior and intermediate lobes with six distinct endocrine cell types at E18.5. The posterior pituitary lobe develops from an evagination of the ventral midline of the forebrain adjacent to the dorsal aspect of Rathke's pouch starting at E10.5. This infundibulum, or neurohypophyseal bud, elongates adjacent to the dorsal roof of the adenohypophysis and its neuroectodermal progenitors differentiate into specialized astroglial cells, collectively referred to as pituicytes. They envelop axonal projections of magnocellular neurosecretory cells of the paraventricular nucleus and the supraoptic nucleus of the hypothalamus, which release the hormones oxytocin (Oxt) and arginine vasopressin (Avp) (for reviews, see Amar and Weiss, 2003; Zhu et al., 2007).

Embryological and genetic experiments have shown that induction, growth and patterning of Rathke's pouch depends on extrinsic cues from the adjacent neuroectoderm (Daikoku et al., 1982; Watanabe, 1982). Bmp4 from the ventral diencephalon induces the formation and initial growth of Rathke's pouch, whereas expansion and maintenance of undifferentiated progenitors in the dorsal region of this tissue is mediated by members of the fibroblast growth factor family (Fgf8, Fgf10 and Fgf18) from the infundibulum (Ericson et al., 1998; Norlin et al., 2000; Treier et al., 1998; Treier et al., 2001). Infundibular Fgfs also counteract the activity of Bmp2 and Shh from the oral roof ectoderm, resulting in the patterning of Rathke's pouch along its dorsoventral axis. An array of transcription factors subsequently orchestrates the position-dependent commitment and differentiation of progenitor cells to the endocrine cell types of the adenohypophysis (Ericson et al., 1998; Treier et al., 1998; for reviews, see Dasen and Rosenfeld, 2001; Zhu et al., 2007).

The molecular control of neurohypophysis development is much less clear. In mice mutant for *Tcf4*, *Sox3* and *Wnt5a*, or conditionally mutant for *Shh* in the hypothalamus, evagination of the primary infundibulum is severely compromised, possibly owing to a failure to restrict expression of *Bmp4* and *Fgf8* in the ventral diencephalon

[1]Institut für Molekularbiologie, Medizinische Hochschule Hannover, 30625 Hannover, Germany. [2]Department of Biochemistry and Molecular Biology, Basic Medical College, Tianjin Medical University, Tianjin 300070, China. [3]Heart Failure Research Center, Academic Medical Center, University of Amsterdam, 1105 AZ Amsterdam, The Netherlands. [4]Perelman School of Medicine at the University of Pennsylvania, Department of Genetics, Philadelphia, PA 19103, USA.

*These authors contributed equally to this work
‡Authors for correspondence (epsteind@mail.med.upenn.edu; kispert.andreas@mh-hannover.de)

Accepted 2 April 2013

(Brinkmeier et al., 2007; Potok et al., 2008; Rizzoti et al., 2004; Zhao et al., 2012). In mice lacking the transcription factor genes *Hesx1*, *Lhx2*, *Nkx2-1* and *Rax*, as well as in *Hes1 Hes5* double mutants, the infundibulum does not form at all (Dattani et al., 1998; Kimura et al., 1996; Kita et al., 2007; Medina-Martinez et al., 2009; Takuma et al., 1998; Zhang et al., 2000; Zhao et al., 2010). How these and other factors are integrated to pattern the diencephalon and direct the localized formation of the infundibulum, and how subsequent differentiation of the neurohypophysis is controlled, are unresolved questions.

Tbx2 and *Tbx3* encode a closely related pair of transcriptional repressors that direct differentiation and patterning processes in the development of numerous vertebrate organs (Naiche et al., 2005). Both genes have recently been shown to be expressed in the ventral diencephalon and the infundibulum (Pontecorvi et al., 2008), but a functional requirement in pituitary development has not been reported. Here, we show that *Tbx3*-deficient mice lack a neurohypophysis and have a degenerated adenohypophysis. We trace these defects to a failure to establish a *Shh*$^{-}$ territory in the ventral diencephalon, and present the molecular mechanisms for repression of *Shh* by Tbx3 in this domain.

MATERIALS AND METHODS

Mice

Mice carrying a null allele of *Tbx2* [*Tbx2*$^{tm1.1(cre)Vmc}$; synonym: *Tbx2*^{cre}] (Aanhaanen et al., 2009) or of *Tbx3* [*Tbx3*$^{tm1.1(cre)Vmc}$; synonym: *Tbx3*^{cre}] (Hoogaars et al., 2007), and the *R26*^{mTmG} reporter line [*Gt(ROSA)26Sor*$^{tm4(ACTB-tdTomato,-EGFP)Luo/J}$; synonym: *Rosa26*^{mTmG}] (Muzumdar et al., 2007) were maintained on an NMRI outbred background. *Tbx2*$^{cre/cre}$ (*Tbx2KO*) and *Tbx3*$^{cre/cre}$ (*Tbx3KO*) embryos were obtained from heterozygous intercrosses. Wild-type littermates were used as controls. *Tbx2*$^{cre/+}$*;R26*$^{mTmG/+}$ embryos (for genetic lineage tracing experiments) were derived from matings of *Tbx2*$^{cre/+}$ males and *R26*$^{mTmG/mTmG}$ females. Pregnant females were sacrificed by cervical dislocation; embryos were harvested in PBS, fixed in 4% paraformaldehyde (PFA)/PBS overnight, and stored in 100% methanol at −20°C until use.

Histological analysis, RNA *in situ* hybridization analysis and cellular assays

Embryos were embedded in paraffin and sectioned at a thickness of 5 or 10 μm. For histological analysis, 5 μm paraffin sections were stained with Hematoxylin and Eosin. RNA *in situ* hybridization analysis on 10 μm paraffin sections was performed following a standard procedure with digoxigenin-labeled antisense riboprobes (Moorman et al., 2001). Cell proliferation rates were investigated by the detection of incorporated 5-bromo-2′-deoxyuridine (BrdU) on 5 μm paraffin sections according to published protocols (Bussen et al., 2004). For each specimen, five adjacent sections were assessed. The BrdU-labeling index was defined as the number of BrdU-positive nuclei relative to the total number of nuclei as detected by DAPI counterstaining. Apoptosis in tissues was investigated by the TUNEL assay using the ApopTag Plus Fluorescein *In Situ* Apoptosis Detection Kit (Chemicon) on 5 μm paraffin sections. All sections were counterstained with DAPI.

Immunofluorescence

For the detection of antigens on 5 μm paraffin sections, the following primary antibodies and dilutions were used: polyclonal rabbit antisera against Oxt (Millipore; 1:200) and Avp (Millipore; 1:200) and monoclonal antibodies from mouse against GFP (Roche; 1:200) and from rat against Emcn (a kind gift of D. Vestweber, Max Planck Institute for Molecular Biomedicine, Münster, Germany; 1:5). Labeling with primary antibodies was performed at 4°C overnight after antigen retrieval (Antigen Unmasking Solution, Vector Laboratories) and incubation in 2.5% normal goat serum in PBST (0.1% Tween-20 in PBS) or blocking solutions provided in the Mouse-on-Mouse Kit (Vector Laboratories). Primary antibodies were visualized with Alexa488- or Alexa555-conjugated secondary antibodies (Invitrogen; 1:200).

Image analysis

Sections were photographed using a Leica DM5000 microscope with Leica DFC300FX digital camera. Laser scanning microscopy was performed for immunofluorescence staining using a Leica TCS SP2 microscope. All images were processed in Adobe Photoshop CS4.

Plasmid construction

A cDNA encoding a Flag-tagged version of human SOX2 was cloned into the *pcDNA3* expression vector (Invitrogen). The cDNA encoding wild-type human HA-tagged TBX2 was described previously (Habets et al., 2002). The *HA-TBX2*$^{\Delta RD}$ deletion construct was generated by removing an internal *Bst*EII fragment encompassing the repression domain of TBX2 (Jacobs et al., 2000). Mutations of *SOX2* and *TBX2* were introduced into wild-type constructs by site-directed mutagenesis using the QuickChange Site-Directed Mutagenesis Kit (Stratagene).

Transient transfection and dual reporter assays

COS-1 cells were cultured under standard conditions in DMEM (GibcoBRL) supplemented with 10% fetal bovine serum, and transfected at 50-70% confluency using FuGENE 6 (Roche Applied Science). Wild-type or mutant *SBE2*-luciferase reporter construct *pGL4.23[luc2/minP]* (1 μg; Promega) was mixed with 2 μg of *Flag-SOX2-pcDNA3* and *HA-TBX2-pcDNA3.1* plasmid in total, or empty vector for compensation, and 5 ng of *pRL-TK* vector (Promega) as an internal control, then applied to cells grown in a 3-cm dish. Cells were harvested 48 hours after transfection and analyzed for firefly and *Renilla* luciferase activities (Dual Luciferase Assay System, Promega). Enhancer activity was expressed as fold induction relative to that of cells transfected with the empty *pcDNA3.1* vector. At least three independent experiments were performed for each construct in triplicate.

Western blot and co-immunoprecipitation

COS-1 cells cultured in 15-cm dishes were transfected with *Flag-SOX2-pcDNA3* or *HA-TBX2*^{wt}/*TBX2*$^{R122E/R123E}$/*TBX2*$^{\Delta RD}$*-pcDNA3.1*, or co-transfected with both in a 1:8 ratio. Forty-eight hours after transfection, cells were washed in cold PBS and transferred to cold lysis buffer (50 mM KCl, 20 mM HEPES, pH 7.9, 2 mM EDTA, 0.1% NP-40, 10% glycerol, 0.5% non-fat milk). The cell lysate was pre-cleared with protein A and G agarose beads (Upstate) by rotating at 4° for 2 hours, then incubated with anti-Flag M2 beads or monoclonal anti-HA Agarose (Sigma) overnight. Beads were washed four times with lysis buffer by rotating for 4-5 minutes at 4° followed by centrifugation at 3000 rpm (956 ***g***) for 3 minutes. After the final wash, the protein beads were spun down at high speed, incubated in 2× sample buffer, boiled, and separated by SDS-PAGE. Western blots were performed as previously described (Zhao et al., 2009).

Chromatin immunoprecipitation (ChIP)

COS-1 cells cultured in a 15-cm dish were co-transfected with an *SBE2*-luciferase reporter construct and one or more of the following: *Flag-SOX2-pcDNA3*, *HA-TBX2*, *TBX2*$^{R122E/R123E}$, *TBX2*$^{\Delta RD}$, *pcDNA3.1*. ChIP experiments were performed essentially as described (Zhao et al., 2012) using antibodies against Flag and HA (Sigma). QPCR was performed as described (Jeong et al, 2008).

Electromobility shift assay (EMSA)

COS-1 cells were transfected with *HA-TBX2*, *TBX2*$^{R122E/R123E}$ or *pcDNA3.1*. Forty-eight hours after transfection, whole-cell lysates were prepared in a RIPA buffer containing 50 mM Tris-HCl, pH 7.5, 150 mM NaCl, 1% Triton X-100 and 0.5% sodium deoxycholate and protease inhibitor cocktail. EMSA was performed as described (Jeong et al., 2008). The sequence of the sense strand of oligonucleotide probes is as follows: consensus T-box site (bold): 5′-CTAGATT**TCACACCT**AGGTGTGAAATCTAG-3′, SBE2 T-box site1 (bold): 5′-ATGGGGGATTA**GCACACGT**TTTCGTCTTAT-3′, SBE2 T-box site mutant (underlined): 5′-ATGGGGGATTA**GCTTA-GCT**TTTCGTCTTAT-3′.

Human *TBX2* and *TBX3* protein with C-terminally fused myc-tag were generated from *pSP64* expression constructs using the TNT-SP6 High-Yield

Wheat Germ Protein Expression System (Promega). *HR-c* and *HR-c(ΔT-Site)* DNA fragments were released as 88-bp *Not*I fragments from reporter plasmids *RC9* and *RC14* (Jeong and Epstein, 2003) and end-labeled with [α-^{32}P]dCTP (Hartmann, Braunschweig, Germany). Binding reactions for EMSAs contained 1-1.5 μl of protein in a total volume of 11 μl of buffer (10 mM Tris, pH 7.2, 100 mM KCl, 1 mM DTT, 10% glycerol) with 1 μl complete protease inhibitor mixture (Roche Applied Science) and 1 μg of double-stranded poly(dI-dC) (Pharmacia). Reactions were pre-incubated for 15 minutes on ice before 4000 counts of probe were added. For supershift experiments, 1 μl of anti-myc antibody (9E10, Sigma) was added to the lysate. Complexes were allowed to form at room temperature for 15 minutes before the reactions were loaded on a native 4% polyacrylamide gel (0.5 M Tris-borate-EDTA). Gels were run at 10 V/cm at 4°C for 5 hours before they were dried and exposed to autoradiography film.

RESULTS

Tbx2 expression marks neurohypophysis progenitor cells within the Tbx3$^+$ ventral midline of the diencephalon

Previous analyses demonstrated co-expression of *Tbx2* and *Tbx3* in the midline of the ventral diencephalon from E9.5 to E15.5. *Tbx2* expression was primarily confined to the infundibulum and later to the neurohypophysis, whereas *Tbx3* expression expanded into the posterior region of the ventral diencephalon. Along the dorsoventral axis, *Tbx2* was limited to cells within the ventral midline, whereas *Tbx3* expression comprised lateral aspects as well. In addition, transient expression of *Tbx2* was observed in mesenchymal cells surrounding the adenohypophysis, which contribute to the hypophyseal portal system, and of *Tbx3* in the ventral aspects of the forming adenohypophysis (Pontecorvi et al., 2008). Our expression analysis by RNA *in situ* hybridization on whole embryos and midsagittal sections of the head from E9.5 to E18.5 confirmed these findings and showed that expression of both genes was maintained in these domains at least until newborn stages (supplementary material Fig. S1).

To analyze whether *Tbx2* expression in the ventral diencephalon is restricted to precursors of the neurohypophysis, we performed *cre*/*loxP*-based genetic lineage tracing using a *cre* knock-in allele of *Tbx2* (*Tbx2^{cre}*) in combination with the sensitive *Rosa26^{mTmG}* reporter line (Aanhaanen et al., 2009; Muzumdar et al., 2007). Reporter activity, as assessed by immunofluorescent detection of GFP in *Tbx2$^{cre/+}$;Rosa26$^{mTmG/+}$* embryos was first observed at E10.5 in ventral midline cells of the diencephalon in a domain adjacent to Rathke's pouch (Fig. 1A-C). In accordance with non-neural expression domains of *Tbx2*, GFP$^+$ cells were also detected in the mesenchymal sheet between the anterior ventral diencephalon and the epithelium of the oral cavity. At E18.5, GFP$^+$ cells were located in the neurohypophysis, including the infundibulum and the pars nervosa (Fig. 1D-F). Co-immunofluorescence with the endothelial marker endomucin (Emcn) (Morgan et al., 1999) demonstrated the contribution of GFP$^+$ cells to the vasculature of the adenohypophysis (Fig. 1G). We conclude that *Tbx2* expression within the ventral diencephalon marks progenitor cells of the neurohypophysis as early as E9.5. *Tbx3* expression encompasses the domain of *Tbx2* but extends more laterally and both anteriorly and posteriorly into the diencephalon.

Tbx2 is dispensable for pituitary development

To study the requirement of *Tbx2* in pituitary development, we maintained a *Tbx2*-null allele (*Tbx2^{cre}*) on an NMRI outbred background that supported viability of homozygous mutant mice (*Tbx2KO*) until shortly after birth. Hematoxylin and eosin (HE) staining of midsagittal sections of E18.5 *Tbx2KO* heads showed a

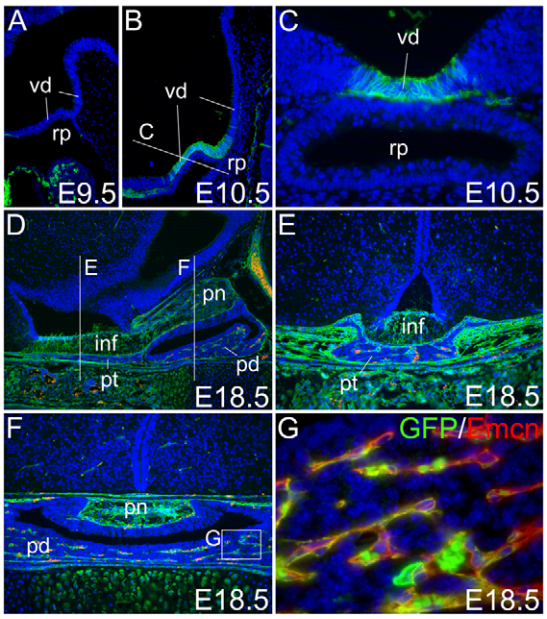

Fig. 1. Genetic lineage tracing of Tbx2$^+$ cells in the developing hypothalamus-pituitary axis. (**A-G**) Immunofluorescent detection of GFP (green) of the *R26^{mTmG}* reporter allele (A-G) and co-staining of Emcn (red) (G) on midsagittal (A,B,D) and coronal sections (C,E,F,G) of *Tbx2$^{cre/+}$;Rosa$^{mTmG/+}$* embryos at the indicated stages. Section planes of C,E,F are indicated by white lines in B,D. The region depicted in G is indicated in F. Blue, DAPI. inf, infundibulum; pd, pars distalis; pn, pars nervosa; pt, pars tuberalis; rp, Rathke's pouch; vd, ventral diencephalon.

pituitary gland that was indistinguishable from control embryos (supplementary material Fig. S2A,A′). To confirm the presence of a functional posterior lobe, we analyzed a set of region- and cell type-specific markers. *In situ* hybridization analysis showed that *cre* (from the mutant allele) was restricted to the posterior lobe of *Tbx2KO* mutants, similar to *Tbx2* in wild-type embryos. Expression of *Cacna1b* (Wang et al., 2009) and *Sox10* (Kuhlbrodt et al., 1998) was detected in pituicytes of both wild-type and *Tbx2KO* embryos. Finally, immunofluorescent detection of Oxt and Avp in *Tbx2* mutants indicated a normal innervation of the neurohypophysis by projections from hypothalamic nuclei (supplementary material Fig. S2B-F′).

As the infundibulum provides essential cues for adenohypophysis development, we investigated the expression of a panel of molecular markers for adenohypophyseal cell lineages. Expression of *Pcsk2* (melanotropes) (Marcinkiewicz et al., 1993), *Pomc* (melanotropes and corticotropes), *Gh* (somatotropes), *Prl* (lactotropes), *Tshb* (thyrotropes) and *Fshb* (gonadotropes) was not changed upon loss of *Tbx2* (supplementary material Fig. S2G-L′). Together, these data suggest that *Tbx2* is dispensable for pituitary development.

Loss of *Tbx3* disturbs pituitary morphogenesis

To investigate the role of *Tbx3* in pituitary development, we performed histological analysis of embryos homozygous mutant for a previously generated *Tbx3*-null allele (*Tbx3$^{cre/cre}$*; synonym: *Tbx3KO*) (Hoogaars et al., 2007) from the onset of pituitary formation at E9.5 to E14.5, i.e. shortly before these embryos die as a result of hepatic and cardiovascular defects (Lüdtke et al., 2009) (Fig. 2). At E9.5, a rudimentary pouch was present, and the ventral diencephalon formed a small kink at its most dorsal position both in wild-type and mutant embryos. In E10.5 wild-type embryos, the

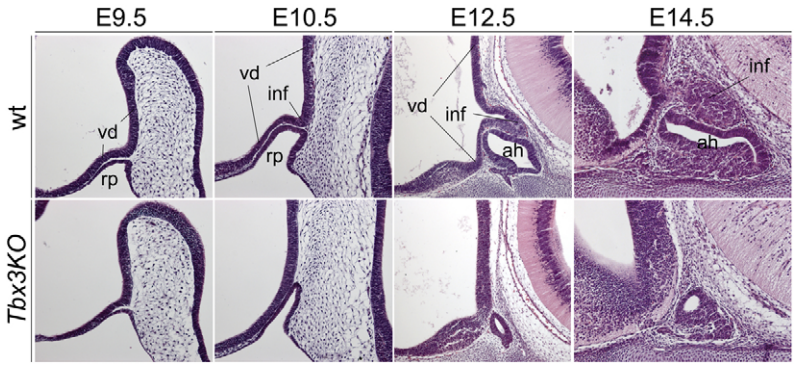

Fig. 2. Loss of *Tbx3* affects morphogenesis of the pituitary gland. Hematoxylin and Eosin staining of midsagittal sections of control (wt) and *Tbx3KO* embryos at the indicated stages. ah, adenohypophysis; inf, infundibulum; rp, Rathke's pouch; vd, ventral diencephalon.

pouch was significantly increased in size compared with a day earlier and featured an almost rectangular shape. The ventral diencephalon had evaginated and formed an infundibulum that extended along the dorsal surface of the pouch. In *Tbx3KO* embryos, the pouch was smaller and the dorsal tip was rounded. The ventral diencephalon adjacent to Rathke's pouch was thickened and lacked any sign of evagination at this or subsequent stages of analysis. Irrespective of the genotype, Rathke's pouch had pinched off the oral surface ectoderm to form the prospective adenohypophysis at E12.5. However, its size and morphological complexity was dramatically reduced at this stage and at E14.5 in *Tbx3KO* embryos (Fig. 2). Transverse sections of the ventral diencephalon at E12.5 confirmed increased stratification of the neuroectoderm in *Tbx3KO*s. The ventral midline in proximity to the adenohypophysis had a normal thickness but showed a reduced mediolateral expansion (supplementary material Fig. S3). We conclude that *Tbx3* is crucial for formation of the infundibulum and the posterior pituitary lobe; hypodysplasia of the adenohypophysis might be secondary to changed signaling upon loss of *Tbx3* in the ventral diencephalon.

Increased cell proliferation in the ventral diencephalon of *Tbx3KO* embryos

Abnormal thickening of the ventral diencephalon, loss of infundibulum formation and hypodysplasia of the adenohypophysis in *Tbx3KO* embryos might result from changed patterns of apoptosis and proliferation during early pituitary development. Apoptosis, as detected by the TUNEL assay, was invariably low in the ventral diencephalon and Rathke's pouch of both wild-type and mutant embryos at E9.5 and E10.5 (Fig. 3A), but was strongly increased in both compartments at E11.5 and E12.5 (supplementary material Fig. S4), arguing against a causative role for the loss of the infundibulum. By contrast, proliferation, as detected by the BrdU incorporation assay, was significantly increased both at E9.5 (1.2-fold) and at E10.5 (3.4-fold) in the ventral diencephalon of *Tbx3KO* embryos. In Rathke's pouch, proliferation was decreased by 15% at E9.5 and by 19% at E10.5 in *Tbx3KO* embryos (Fig. 3B,C).

As *Tbx3* had been implicated in the control of cell cycle progression in previous studies (for a review, see Lu et al., 2010), we analyzed by *in situ* hybridization analysis the expression of a number of genes encoding cell-cycle regulators at E10.5. We failed to detect expression of the genes of the anti-proliferative factors *Cdkn1a* (*p21*), *Cdkn1b* (*p27*), *Cdkn2a* (*p16* and *p19ARF*), *Cdkn2b* (*p15*), *Cdkn2c* (*p18*) and *Cdkn2d* (*p19*) in the ventral diencephalon of both wild-type and *Tbx3KO* embryos at this stage (supplementary material Fig. S5). *Cdkn1c* (*p57*) was expressed in the posterior ventral diencephalon, including the infundibulum region, in wild-type embryos. In the diencephalon of *Tbx3KO* embryos, *Cdkn1c* expression was restricted to a smaller domain adjacent to the tip of Rathke's pouch. Interestingly, we found strong ectopic expression of the pro-proliferative genes *Mycn* and *Ccnd2* in the posterior ventral diencephalon of *Tbx3KO* embryos, whereas expression of these genes was restricted to small domains in the posterior diencephalon at the level of the mammillary recess in the wild type. Expression of *Ccnd1* in the posterior ventral diencephalon was unchanged in the mutant (Fig. 3D). Hence, Tbx3 controls expression of cell-cycle regulators in the ventral diencephalon to restrict cell proliferation in this domain.

Loss of *Tbx3* affects growth and patterning of the developing adenohypophysis

To address further how the loss of *Tbx3* affects the development of the adenohypophysis, we analyzed the expression of a panel of marker genes associated with growth, patterning and differentiation of this tissue by *in situ* hybridization at E10.5, E12.5 and E14.5 (Fig. 4).

Lhx3, *Six3* and *Pax6* have been implicated in survival and proliferation of precursor cells and establishment of dorsal cell fates, respectively, in the developing adenohypophysis (Gaston-Massuet et al., 2008; Kioussi et al., 1999; Sheng et al., 1996; Zhao et al., 2006). At E10.5, the three genes were co-expressed in the dorsal-most two-thirds of Rathke's pouch in wild-type embryos. In *Tbx3KO* embryos, *Lhx3* expression was unchanged whereas expression of *Six3* and *Pax6* was absent. In E12.5 wild-type embryos, *Lhx3* was expressed in the entire adenohypophysis, *Nkx3-1* was restricted to the most dorsal aspect, and *Aldh1a2* (also known as *Raldh2*) was expanded ventrally. *Pou3f4* (also known as *Brn4*) was found in an intermediate region overlapping with the ventral domain of *Aldh1a2* but was excluded from the most ventral aspect of the adenohypophysis, which was positive for *Gata2* and *Foxl2*. In *Tbx3*-deficient embryos, *Lhx3* expression was preserved. *Nkx3-1* and *Aldh1a2* expression was completely abolished whereas *Pou3f4* expression was expanded to cover all cells of the rudimentary adenohypophysis excluding the most ventral aspect, which still maintained normal expression of *Gata2* and *Foxl2* (Fig. 4). At E14.5, expression of *Tbx19* (also known as *Tpit*), *Pou1f1* (also known as *Pit1*) and *Cga* marks common progenitor pools for the corticotrope/melanotrope, the lactotrope/somatotrope/thyrotrope and the thyrotrope/gonadotrope lineages, respectively, which are thought to be established from dorsal, intermediate and the most ventral precursor cells in the developing adenohypophysis (for reviews, see Dasen and Rosenfeld, 2001; Scully and Rosenfeld, 2002). In *Tbx3KO* embryos, expression of *Tbx19* and *Pou1f1* was abolished and strongly reduced, respectively, whereas expression of *Cga* was unchanged,

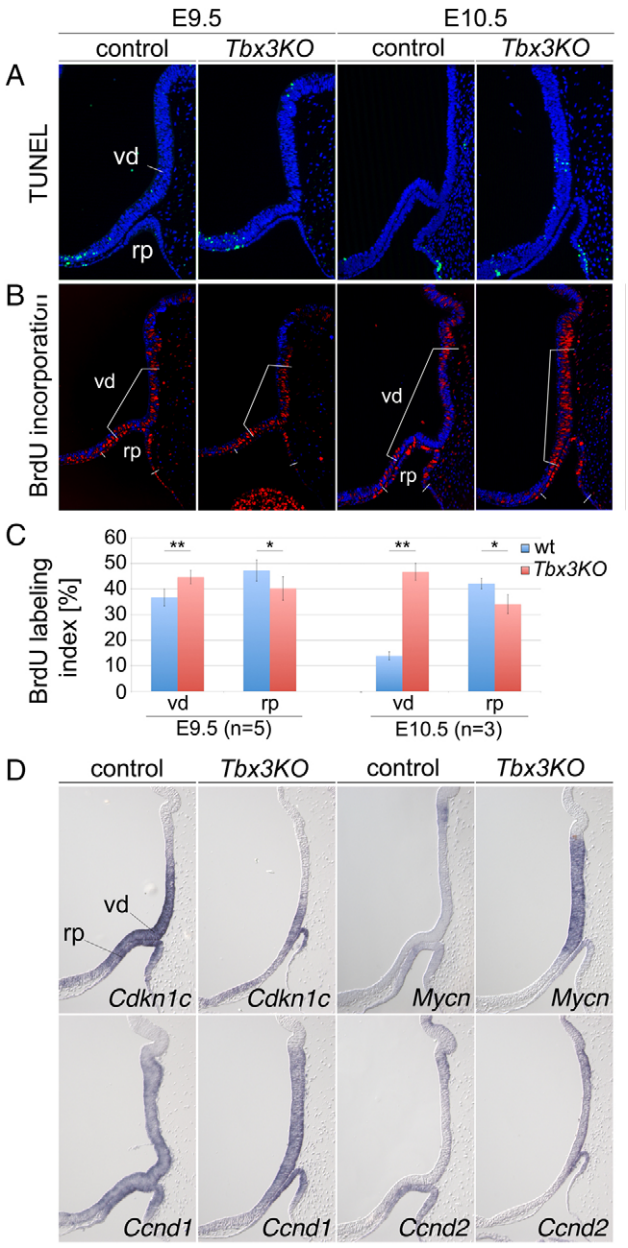

Fig. 3. The ventral diencephalon is hyperproliferative in *Tbx3*-deficient embryos. (**A**,**B**) Analysis of cell death by the TUNEL assay (A) and of cell proliferation by the BrdU incorporation assay (B) on midsagittal sections of control and *Tbx3KO* embryos. Cranial is to the left. Stages are as indicated in the figure. (B) False color overlay of DAPI (blue) and BrdU signals (red). The domains analyzed for proliferation correspond to the *Tbx3* expression domain and are labeled within the figures. (**C**) Quantification of BrdU-positive cells. E9.5 (n=5), wild type (wt) versus mutant: vd: 36.7±3.3% versus 44.7±2.7%, P=0.003; rp: 47.2±4.1% versus 40.2±4.6%, P=0.036. E10.5 (n=3), wild type versus mutant: vd: 13.9±1.6% versus 46.7±3.3%, P=0.0001; rp: 42.1±2.1% versus 34.1±3.7%, P=0.03. Error bars indicate s.d. *P<0.05; **P<0.01; two-tailed Student's t-test. (**D**) *In situ* hybridization analysis on midsagittal sections of E10.5 control and *Tbx3KO* embryos. rp, Rathke's pouch; vd, ventral diencephalon.

indicating the presence of ventral cell lineages only (Fig. 4). We conclude that *Tbx3* and *Tbx3*-dependent signals from the ventral diencephalon are required to establish dorsal cell fates and lineages in the developing adenohypophysis.

Disturbed anterior-posterior patterning of the ventral diencephalon in *Tbx3KO* embryos

Lack of infundibulum formation might reflect the specific loss of primordial segments along the anterior-posterior axis of the ventral diencephalon. To investigate such patterning defects, we analyzed a panel of marker genes that show restricted expression in the ventral diencephalon and/or are required for normal development of the neurohypophysis. At E10.5, i.e. at a stage when the morphological changes in the ventral diencephalon were fully apparent, expression of the transcription factor genes *Nkx2-1*, *Emx2*, *Otx2*, *Sox2*, *Sox3*, *Six3*, *Lhx2*, *Six6* and *Rax* (Brinkmeier et al., 2007; Furukawa et al., 1997; Jean et al., 1999; Kelberman et al., 2006; Mathers et al., 1997; Oliver et al., 1995; Rizzoti et al., 2004; Simeone et al., 1993; Simeone et al., 1992; Takuma et al., 1998; Zhao et al., 2010) was unchanged in *Tbx3KO* embryos (supplementary material Fig. S6). *Cre* expression from the mutant allele was established in *Tbx3KO* embryos, but appeared to be diminished compared with $Tbx3^{cre}$ control embryos; *Pou3f4* and *Hes5* (Alvarez-Bolado et al., 1995; Hatakeyama et al., 2004; Kita et al., 2007) were ectopically expressed in this region (Fig. 5). By contrast, expression of *Tbx2*, which marks the prospective neurohypophysis in the wild type, was abolished in the ventral diencephalon of mutant embryos, indicating that *Tbx3* is required for formation of the $Tbx2^{+}$ infundibulum subdomain.

We next analyzed expression of components of signaling pathways that may account for the observed patterning defects and cellular changes in both the ventral diencephalon and the adenohypophysis of *Tbx3*-deficient embryos. *Fgf8*, *Fgf10* and *Bmp4* are expressed in the posterior ventral diencephalon, including the infundibulum, at E10.5 in the wild type (Ericson et al., 1998; Treier et al., 2001). In *Tbx3KO* embryos, *Fgf8* and *Bmp4* expression was normal, but *Fgf10* expression was clearly downregulated. Interestingly, *Shh* was ectopically expressed in the ventral midline of the anterior diencephalon (Echelard et al., 1993). Ectopic expression of *Ptch1*, a transcriptional downstream target of the Shh pathway (Ågren et al., 2004; Vokes et al., 2007), confirmed that de-repression of *Shh* is associated with enhanced signaling activity of this pathway in the midline of the ventral diencephalon in *Tbx3KO* embryos.

To distinguish primary from secondary changes, we analyzed expression of the genes altered at E10.5 in the ventral diencephalon at E9.5, i.e. before infundibulum formation occurs. Expression of *Fgf8*, *Fgf10* and *Bmp4* was unchanged at this stage whereas ectopic expression of *Pou3f4*, *Hes5*, *Shh* and *Ptch1* and loss of *Tbx2* expression preceded the morphological and histological changes in the *Tbx3*-deficient ventral diencephalon. As repression of *Tbx2* and induction of *Pou3f4* by Shh has been suggested in other developmental contexts (Riccomagno et al., 2002; Zhao et al., 2012), we assume that these changes are subordinate to altered activity of the Shh pathway in the ventral diencephalon of *Tbx3KO* embryos.

TBX3 inhibits SOX2 from activating *SBE2*

Shh brain enhancer-2 (*SBE2*) is a long-range acting regulatory element that controls the expression of *Shh* in the rostral diencephalon, including its repression from the ventral midline at the level of the infundibulum (Jeong et al., 2006). *Shh* transcription in the rostral diencephalon is dependent on several transcription factors, including Sox2 and Sox3, which directly bind to and activate *SBE2* (Zhao et al., 2012). To determine how Tbx3 mediates its repressive effects on *Shh* transcription, we performed a series of co-transfection experiments in COS-1 cells with wild-type and mutant forms of human SOX2 and TBX2/3 (Fig. 6A). As previously demonstrated, SOX2 is a potent activator of *SBE2*-luciferase expression (Zhao et

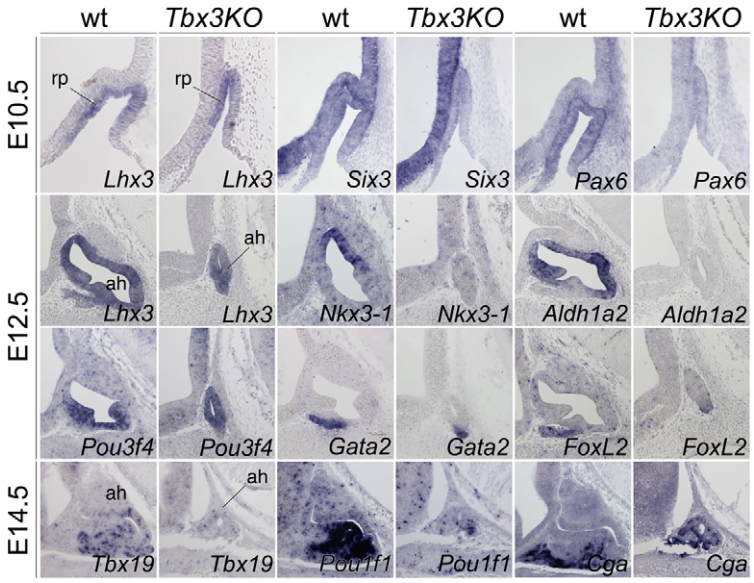

Fig. 4. Molecular analysis of the developing adenohypophysis in *Tbx3KO* embryos. *In situ* hybridization analysis on midsagittal sections of control (wt) and *Tbx3KO* embryos at the indicated stages. Cranial is to the left. ah, adenohypophysis; rp, Rathke's pouch.

al., 2012; Fig. 6B). By contrast, TBX3 (or TBX2) had no effect on *SBE2* when transfected on its own (Fig. 6B). However, in the presence of both SOX2 and TBX3 (or TBX2), there was a significant reduction in *SBE2*-luciferase activity, compared with SOX2 alone (Fig. 6B) suggesting that repression of *Shh* transcription by Tbx3 results from inhibition of *SBE2* activation by Sox2.

Tbx and Sox proteins are known to interact with a variety of protein partners, including each other (Boogerd et al., 2011; Habets et al., 2002; Reményi et al., 2003). To determine whether SOX2 and TBX2/3 can physically interact, we performed co-immunoprecipitation (co-IP) experiments. Given the high degree of homology between TBX2 and TBX3, the availability of already existing TBX2 variants, and the finding that Tbx2 can repress *Shh* in chick embryos, all subsequent experiments were performed with TBX2 (Lingbeek et al., 2002; Manning et al., 2006). COS-1 cells were transfected with constructs encoding Flag-tagged SOX2, Hemagglutinin (HA)-tagged TBX2 and/or empty vector (Fig. 6A,C). Western blot analysis demonstrated that the anti-HA antibody was able to immunoprecipitate SOX2 and the anti-Flag antibody was able to immunoprecipitate TBX2, suggesting a physical association between SOX2 and TBX2 (Fig. 6C).

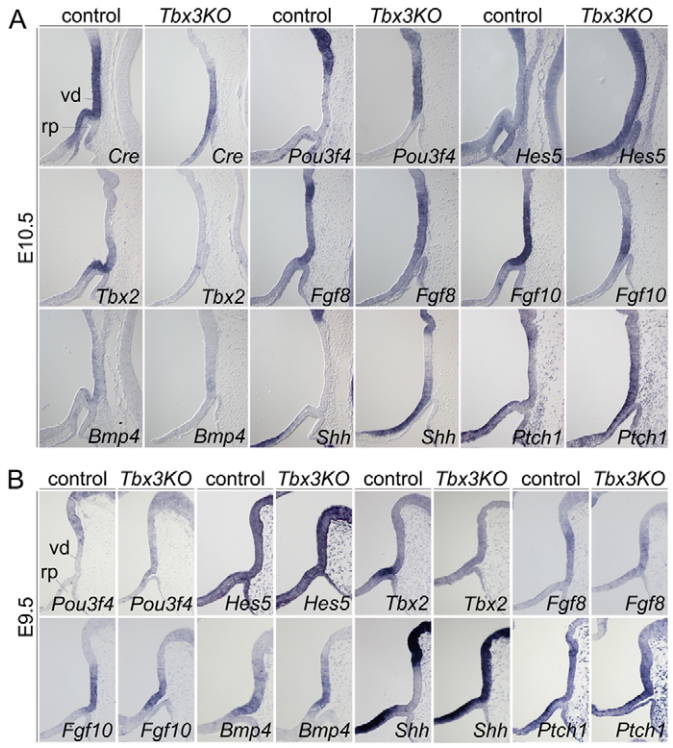

Fig. 5. Molecular analysis of the developing ventral diencephalon in *Tbx3KO* embryos. *In situ* hybridization analysis on midsagittal sections of E10.5 (**A**) and E9.5 (**B**) control and *Tbx3KO* embryos. Cranial is to the left. rp, Rathke's pouch; vd, ventral diencephalon.

Additional co-IP experiments were performed to identify the domains within each protein that are required for their interaction. Three residues at the C-terminus of the SOX2-HMG domain were previously shown to be involved in ternary complex formation with other co-factors (Reményi et al., 2003) (Fig. 6A). To determine whether the same residues are needed for binding with TBX2, constructs carrying mutations in each of them were used in co-IP experiments. Although $SOX2^{R100E/M104E}$ and $SOX2^{R115E}$ maintained their ability to interact with TBX2, a construct containing mutations in all three residues, $SOX2^{R100E/M104E/R115E}$, did not associate with TBX2 (Fig. 6D).

Key residues in the T-box domain of TBX2 (Arg122/Arg123) are crucial for its DNA-binding activity (Habets et al., 2002; Sinha et al., 2000). Interestingly, SOX2 did not pull down $TBX2^{R122E/R123E}$, suggesting that these residues constitute a previously unappreciated protein-interaction domain (Fig. 6E, lane 4). In addition to the T-box domain, the C-terminal repression domain of TBX2 was also required for interaction with SOX2 (Fig. 6E, lane 6).

The domains of TBX2 that interact with SOX2 are also needed to repress *SBE2* activation by SOX2 (Fig. 6F). Whereas wild-type TBX2 repressed the SOX2-dependent activation of *SBE2* in a dose-dependent manner, neither $TBX2^{R122E/R123E}$ nor $TBX2^{\Delta RD}$ impeded SOX2 from activating *SBE2*, even when co-transfected at a much higher ratio (Fig. 6F). Taken together, our results indicate that TBX2/3 can repress *SBE2* activation by SOX2 and that this repression might depend on physical interactions between the two proteins.

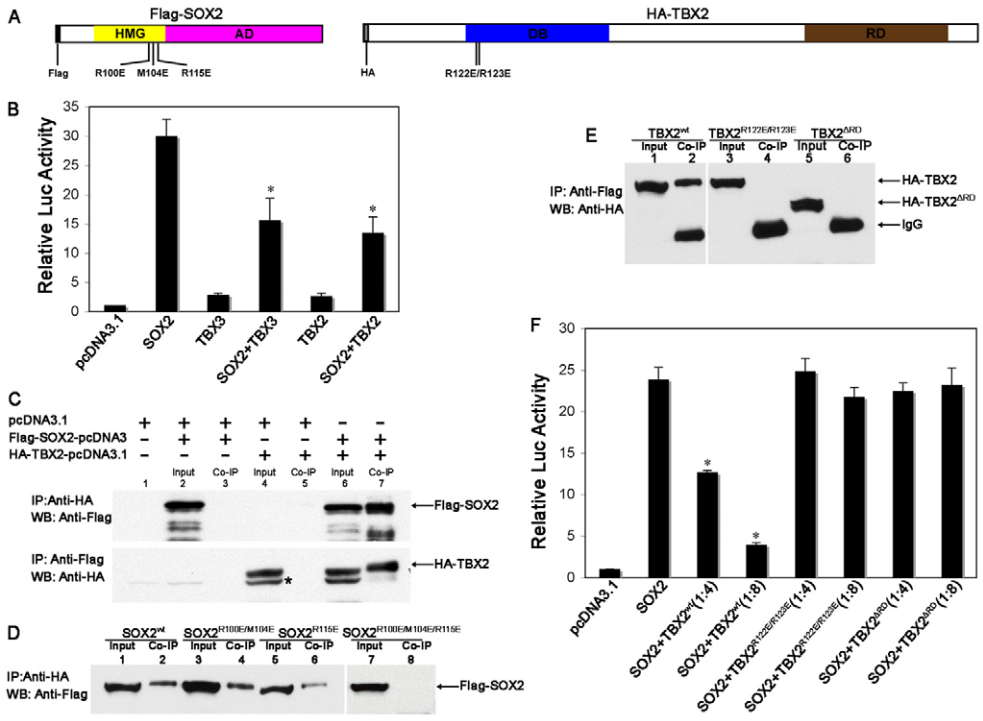

Fig. 6. TBX2 and TBX3 repress *SBE2* activation by SOX2. (**A**) Schematic of Flag-tagged SOX2 and HA-tagged TBX2 showing the position of functional domains: SOX2, high mobility group/DNA-binding domain (HMG), activation domain (AD); TBX2, T-box DNA-binding domain (DB), repression domain (RD), as well as site mutations. (**B**) Luciferase reporter assays performed in COS-1 cells co-transfected with *SBE2*-luciferase and expression constructs for SOX2, TBX2/3 or both. Asterisk indicates statistically significant differences from transfections with SOX2 alone ($P<0.05$, Student's *t*-test). (**C**) Co-IP experiments with Flag-tagged SOX2 and HA-tagged TBX2 normalized for equivalent expression levels in COS-1 cells (lanes 6, 7). The empty vector (*pcDNA3.1*) serves as a negative control (lanes 1-5). Input lanes (2, 4, 6) serve as positive controls. IPs were performed with an anti-HA antibody (upper panel), followed by western blot (WB) with an anti-Flag antibody, or vice versa (lower panel). (**D**) Co-IP experiments with Flag-tagged SOX2 containing different point mutations in the HMG domain (R100E/M104E; R115E; or R100E/M104E/R115E) and HA-tagged TBX2, co-transfected in COS-1 cells. Co-IP was performed with anti-HA antibody followed by western blot with anti-Flag antibody. (**E**) Co-IP experiments with HA-tagged TBX2 containing mutations in the DNA-binding domain (R122E/R123E) or a deletion of the repression domain (ΔRD) and Flag-tagged SOX2 expressed in COS-1 cells. Co-IP experiments were performed with an anti-Flag antibody followed by western blot with an anti-HA antibody. (**F**) Luciferase reporter assays performed in COS-1 cells co-transfected with *SBE2*-luciferase and expression constructs for SOX2, and different variants of TBX2 that disrupt complex formation with SOX2. Error bars in all graphs represent s.e.m.

TBX2/3 disrupts the binding of SOX2 to *SBE2*

In order to clarify the mechanism by which TBX2/3 prevents SOX2 from activating *SBE2*, it was important to know whether TBX2/3 binds directly to *SBE2* and, if so, what impact this might have on SOX2 activator function. We first addressed this question by performing chromatin immunoprecipitation (ChIP) followed by quantitative PCR (QPCR) to evaluate the extent of SOX2 and TBX2 recruitment to *SBE2*. COS-1 cells transfected with SOX2 and *SBE2* showed significant enrichment of *SBE2* DNA overlapping the previously characterized SOX2-binding site, in SOX2- versus IgG-bound chromatin (Fig. 7A) (Zhao et al., 2012). A similar region of *SBE2* DNA was also significantly enriched in TBX2-bound chromatin in COS-1 cells transfected with TBX2 and *SBE2* (Fig. 7A). Remarkably, the recruitment of SOX2 and TBX2 to *SBE2* was completely abolished in COS-1 cells co-transfected with SOX2 and TBX2 (Fig. 7A). Mutations in TBX2 that blocked its interaction with SOX2 did not compromise the binding of SOX2 to SBE2 (Fig. 7A). Thus, Tbx2/3 might repress *Shh* transcription by interfering with Sox2 binding to its target recognition sequence in *SBE2*.

As the TBX2 mutations that disrupt contact with SOX2 also compromise other important aspects of TBX2 function, including DNA binding (R122E/R123E) and co-repressor recruitment (ΔRD), it remained uncertain whether ternary complex formation (TBX2-SOX2-*SBE2*) was a necessary prerequisite for TBX2/3-mediated repression of *Shh*. Based on the ChIP data, TBX2 is recruited to *SBE2*. We next set out to determine whether TBX2 binds directly to *SBE2*. The 750-bp *SBE2* sequence was scanned for T-box binding sites using the rVista tool, but no sequences perfectly matching the consensus were found. After relaxing the stringency to include one or two nucleotide mismatches, two imperfect T-box sites were identified 8 and 30 nucleotides upstream of the Sox2-binding site (Fig. 7B).

We determined binding of TBX2 to either of these putative sites by EMSA. A specific protein-DNA complex was observed when a radiolabeled probe overlapping T-box site1, but not site2, was incubated with COS-1 cell lysates transfected with HA-TBX2^{wt} (Fig. 7B; data not shown). This complex showed a similar mobility shift to that formed between TBX2 and a probe matching a consensus T-box binding site (Fig. 7B). No such complex formed in the presence of the DNA binding-defective TBX2$^{R122E/R123E}$ mutant (Fig. 7B). The specificity of this interaction was further confirmed by super-shifting the TBX2-*SBE2* complex, albeit partially, with an anti-HA antibody (Fig. 7B).

Mutations in *SBE2* T-box site1 did not interfere with the binding of SOX2 on its own, but did prevent TBX2 from binding *SBE2* (Fig. 7C). Despite being unable to bind *SBE2*, TBX2 still blocked the recruitment of SOX2 to *SBE2* (Fig. 7C). Moreover, the absence

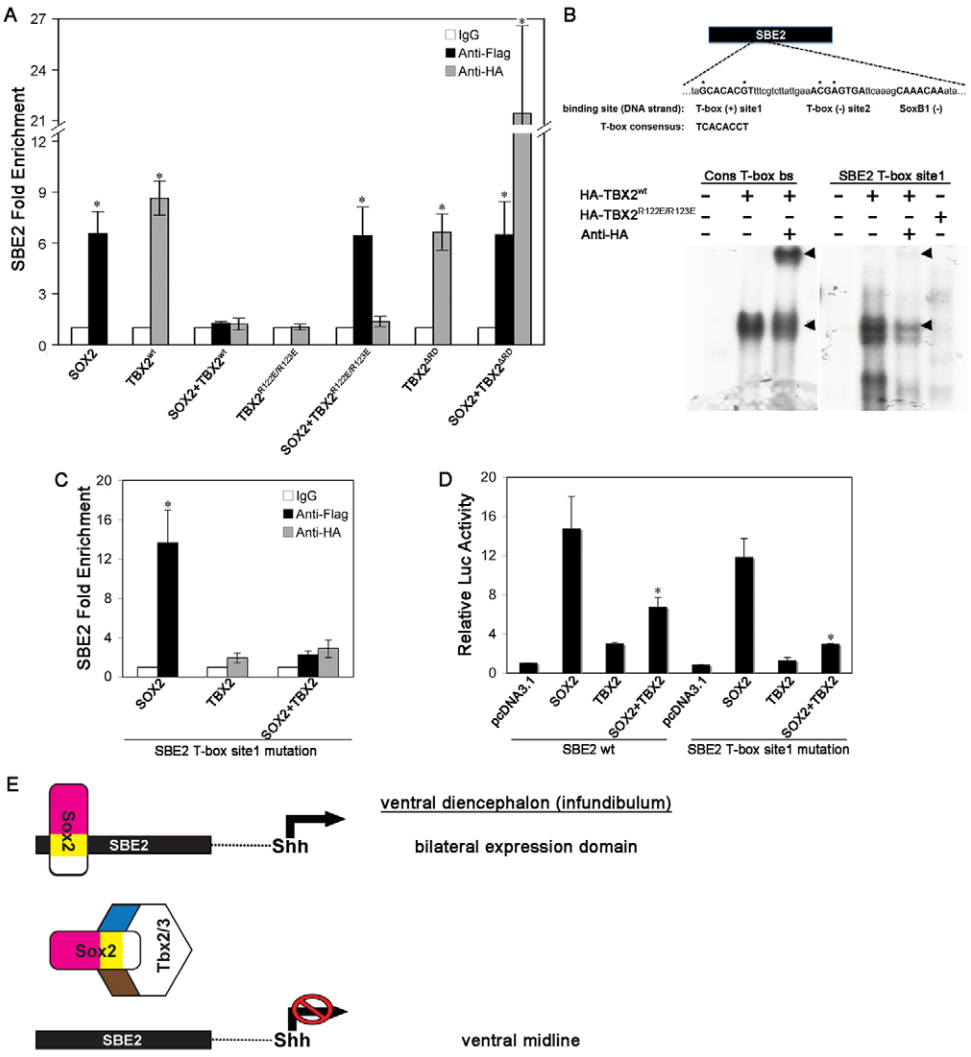

Fig. 7. SOX2 binding to *SBE2* is blocked by TBX2. (**A**) ChIP-QPCR results from COS-1 cells co-transfected with an *SBE2*-luciferase construct and either Flag-tagged SOX2, isoforms of HA-tagged TBX2, or both. QPCR results from three independent experiments reveal a significant enrichment of *SBE2* DNA in SOX2 (black)- and TBX2^{wt} (gray)-bound chromatin when transfected independently, but not together, compared with IgG controls (white) (Student's *t*-test, **P*<0.05). TBX2$^{R122E/R123E}$ was not recruited to *SBE2* and had no influence on SOX2 binding. TBX2$^{\Delta RD}$ was enriched on *SBE2* but did not affect SOX2 recruitment. (**B**) Top: Schematic showing position of candidate T-box binding sites in *SBE2* in relation to the Sox2 site (SoxB1). Asterisk marks nucleotide mismatches with T-box consensus sequence. Bottom: EMSAs performed with COS-1 cell extracts transfected with HA-tagged TBX2 or TBX2$^{R122E/R123E}$ (negative control) and radiolabeled probes overlapping a consensus T-box binding site (Cons T-box bs) or candidate *SBE2* T-box site1. TBX2 complexes migrate similarly when bound to T-box bs or *SBE2* T-box site1 (lower arrowheads). Supershifted complexes form in the presence of anti-HA antibody (upper arrowheads). (**C**) ChIP-QPCR results from COS-1 cells co-transfected with an *SBE2*-luciferase construct containing mutations in T-box site1 and Flag-tagged SOX2 (black), HA-tagged TBX2 (gray) or both. (**D**) Luciferase reporter assays performed in COS-1 cells co-transfected with *SBE2*-luciferase constructs (wt, or *SBE2* T-box site1 mutation), and expression constructs for SOX2, TBX2 or both. Asterisk indicates statistically significant differences from transfections with SOX2 alone (*P*<0.05, Student's *t*-test). (**E**) Schematic showing the transcriptional regulation of *Shh* in the infundibular region of the ventral diencephalon. For details see text.

of *SBE2* T-box site1 did not impede TBX2 from repressing SOX2-dependent *SBE2*-luciferase activity (Fig. 7D). These results indicate that although TBX2/3 binds *SBE2* directly, this binding is not required for TBX2/3 to sequester SOX2 from *SBE2*.

In summary, *Shh* expression in the ventral diencephalon is regulated, in part, by SoxB1 (Sox2/3) transcription factors, which directly bind and activate *SBE2*, a long-range *Shh* forebrain enhancer (Fig. 7E). However, for the pituitary to develop properly, *Shh* transcription must also be extinguished in the ventral midline at the level of the infundibulum. Tbx3 mediates this repression of *Shh* by physically associating with Sox2 and blocking its recruitment to *SBE2* (Fig. 7E).

DISCUSSION

Repression of *Shh* by Tbx2/3 is crucial for infundibulum formation

The infundibulum forms in a highly localized manner from a subregion of the ventral diencephalon. The molecular mechanisms that pattern the ventral diencephalon to drive this dynamic morphogenetic process have been poorly defined. Our analysis has shown that the neurohypophysis derives from a Tbx2^{+}Shh^{-} subdomain within the ventral diencephalon. Although expression of *Tbx3* (and hence *cre* from the *Tbx3^{cre}* allele) in the inner cell mass prevented us from using a conditional approach to test directly the functional significance of ectopic Shh signaling in the *Tbx3*-

deficient ventral diencephalon, a number of findings suggest that repression of *Shh* by Tbx2/3 is crucial for the formation of the infundibulum.

First, upon conditional deletion of *Shh* in the diencephalon of *SBE2-cre;Shh$^{flox/flox}$* mice, the infundibulum exhibits an ectopic, anteriorly shifted position coinciding with an anterior expansion of *Fgf10*, *Bmp4* and *Tbx2* and a reduction of the *Shh^{+}Six6^{+}* domain in the ventral diencephalon (Zhao et al., 2012). Therefore, loss of *Tbx2* in *Tbx3KO* embryos is a likely consequence of ectopic Shh signaling. We cannot exclude a direct regulation, i.e. activation, of *Tbx2* by Tbx3. However, as Tbx3 is described as a transcriptional repressor (Brummelkamp et al., 2001), we deem it unlikely.

Second, Shh has been implicated in mitogenic responses in many developmental contexts (Ishibashi and McMahon, 2002; Wang et al., 2010), in some of which increased proliferation was promoted by upregulation of the proto-oncogene *Mycn* and the G1-cyclin gene *Ccnd2* (Kenney et al., 2003; Mill et al., 2005). Previous *in vitro* and *in vivo* analyses showed that Tbx2 and Tbx3 mediate cell-cycle progression through repression of cell-cycle dependent kinase inhibitor genes of the Cdkn1 and Cdkn2 families (Lingbeek et al., 2002; Lüdtke et al., 2013). However, we did not detect upregulation of any of these family members in the mutant diencephalon but rather found repression of *Cdkn1c* and upregulation of the Shh target genes *Mycn* and *Ccnd2*. The correlation of increased proliferation and lack of infundibulum formation in *Tbx3*-deficient embryos does not support a concept that this morphogenetic process is solely driven by the localized increase of cell proliferation. We suggest that coordinated changes of cell shapes could be a crucial factor in initiation of infundibulum formation, and that these tissue changes are disturbed in *Tbx3KO* embryos, possibly owing to Shh-induced overproliferation.

A crucial requirement for a T-box function to repress *Shh* in the ventral diencephalon was also reported in the chick. However, prolonged activation of Shh signaling in this domain in the chick resulted in growth arrest and prevented progression of floor plate cells to proliferative *Emx2^{+}* hypothalamus progenitor cells but a pituitary defect was not reported (Manning et al., 2006). This suggests that the cellular and molecular programs regulated by Tbx2, Tbx3 and Shh in the ventral diencephalon may have diverged in birds and mammals.

Previous studies showed that mice mutant for *Hesx1*, *Lhx2*, *Nkx2-1* and *Rax*, as well as mice double mutant for *Hes1* and *Hes5* do not form the infundibulum, whereas loss of *Tcf4*, *Sox3* or *Wnt5a* is associated with impaired infundibulum evagination (Dattani et al., 1998; Kimura et al., 1996; Kita et al., 2007; Medina-Martinez et al., 2009; Takuma et al., 1998; Zhang et al., 2000; Zhao et al., 2010). As we did not detect changed expression of *Lhx2*, *Nkx2-1*, *Rax*, *Tcf4* or *Sox3* in *Tbx3KO* embryos, *Tbx3* probably acts downstream of these genes or in a parallel pathway to regulate infundibulum morphogenesis.

Secondary changes in adenohypophysis development

In *Tbx3KO* embryos, Rathke's pouch formed, grew and detached normally from the oral roof ectoderm, compatible with our finding that expression of *Bmp4*, the crucial factor for induction of Rathke's pouch (Takuma et al., 1998), and of *Fgf8* and *Fgf10*, which mediate expansion of precursor cells in the dorsal pouch (Ericson et al., 1998), were established normally at E9.5. However, we observed reduced *Fgf10* expression at E10.5, and ectopic expression of *Ptch1*, the target of Shh signaling in the dorsal aspect of Rathke's pouch at E9.5 and E10.5 (Fig. 5). Subsequent changes in growth (reduced proliferation, increased apoptosis), patterning and differentiation of the developing adenohypophysis (loss of dorsal cell lineages and expansion of ventral intermediate fates) might therefore result from the lack of an infundibular source of Fgf signals as well as from ectopic Shh signals from the ventral diencephalon. In fact, loss of Fgf signaling results in increased apoptosis (De Moerlooze et al., 2000; Ohuchi et al., 2000), whereas overexpression of *Shh* in the developing adenohypophysis causes an expansion of ventral cell lineages and overexpression of the Shh antagonist Hhip in the oral ectoderm in transgenic mice results in loss of the ventral *Gata2^{+}* and *Pou3f4^{+}* cell lineages of the adenohypophysis (Treier et al., 2001). Although mostly associated with pro-proliferative effects (Treier et al., 2001; Wang et al., 2010), abundant Shh signaling may also elicit apoptosis in some developmental contexts (Oppenheim et al., 1999).

As *Tbx3* expression is not restricted to the ventral diencephalon but also occurs in the ventral aspects of Rathke's pouch and the developing adenohypophysis, the observed changes might derive (at least partly) from a cell- and/or tissue-autonomous requirement for *Tbx3* in the adenohypophysis. However, the selective loss of dorsal cell lineages and the maintenance of the ventral most cell fates argues against this possibility.

Repression of *Shh* expression in the ventral diencephalon by DNA-dependent and DNA-independent activities of Tbx2 and Tbx3

Between E8.5 and E9.0, *Shh* is expressed in a continuous band of ventral midline cells of the CNS reaching from the rostral diencephalon to the spinal cord. Expression intensifies and extends into the more rostral aspects of the forebrain until E9.5, but then becomes specifically excluded from the ventral midline and confined to two adjacent ventrolateral stripes in the posterior diencephalon (Echelard et al., 1993). Transgenic reporter assays showed that this complex and dynamic expression pattern results from the combinatorial activity of multiple distinct cis-regulatory elements spread in and around the *Shh* locus. *Shh floor plate enhancer 1* and *2* (*SFPE1*, *SFPE2*) were found to mediate expression in the hindbrain and the spinal cord, *Shh brain enhancer 1* (*SBE1*) in the midbrain and caudal diencephalon, *SBE2* and *SBE4* in the ventral diencephalon and *SBE3* and *SBE4* in the ventral telencephalon. Members of several transcription factor families, including forkhead (Foxa1, Foxa2), homeobox (Nkx2-1, Six3) and Sox-type HMG-domain proteins (Sox2, Sox3) have been identified as positive regulators of *Shh* expression in the CNS via binding to these elements (Epstein et al., 1999; Jeong et al., 2006; Jeong and Epstein, 2003; Jeong et al., 2008; Zhao et al., 2012). The identification of an evolutionary conserved T-box transcription factor binding site (T-site) within *SFPE2*, deletion of which leads to ectopic reporter activation in the ventral midline of the diencephalon, indicated the contribution of T-box transcriptional repressors to the *Shh* expression pattern as well (Jeong and Epstein, 2003).

Our molecular characterization of *Tbx2*- and *Tbx3*-deficient mice identified Tbx3, and not Tbx2 as in the chick, as the crucial factor for *Shh* repression in this domain (Manning et al., 2006). However, Tbx2 and Tbx3 might actually act redundantly in this context in the mouse as *Tbx2* is lost in the *Tbx3*-deficient ventral diencephalon. Further support for this notion derives from the finding that Tbx2 and Tbx3 behave in an equivalent fashion with respect to their DNA-binding and protein-interaction properties (for reviews, see Lu et al., 2010; Plageman and Yutzey, 2005).

Our experiments identified a novel biochemical mechanism for transcriptional repression by Tbx2 and Tbx3 that is independent

from direct binding to DNA via the T-box but relies on protein interaction by the same domain to sequester the transcriptional activators Sox2 and Sox3 from their binding site in the *SBE2* element. Such a DNA-independent function of T-box proteins is not without precedence. In fact, we and others have recently shown that Tbx1 and Tbx20, two related members of the Tbx1 subfamily, attenuate Bmp signaling by sequestering Smad1, Smad5 and Smad8 (Smad9 – Mouse Genome Informatics) from binding to Smad4 (Fulcoli et al., 2009; Singh et al., 2009).

Repression of *Shh* expression in the midline of the ventral diencephalon may not only rely on protein interaction but may additionally utilize the conserved DNA-binding activity of Tbx2 and Tbx3. In fact, in an EMSA with *in vitro* translated myc-tagged TBX2 and TBX3 protein and an 88-bp DNA fragment of *SFPE2* (also termed homology region c, *HR-c*) that harbors the identified T-site (Jeong and Epstein, 2003) as a probe, we found binding of both proteins to this fragment but not to one with a mutated T-site, indicating that Tbx2 and Tbx3 might regulate *Shh* expression in this region by direct transcriptional repression (supplementary material Fig. S7).

To this point, we cannot formally distinguish whether *Shh* repression *in vivo* relies on DNA-dependent (via *SBE2*) and/or on DNA-independent (via *SFPE2*) mechanisms. An answer to this question may derive from analysis of *SFPE2* and *SBE2* reporter expression in a *Tbx3*-deficient background. However, given the severe consequences of a failure in downregulating *Shh* in the midline of the ventral diencephalon, we assume that *in vivo* both mechanisms cooperate to ascertain *Shh* repression.

Acknowledgements
We thank Marianne Petry for technical help.

Funding
This work was supported by the German Research Council (Deutsche Forschungsgemeinschaft, DFG) for the Cluster of Excellence REBIRTH (From Regenerative Biology to Reconstructive Therapy) at Medizinische Hochschule Hannover; and by internal grants from Medizinische Hochschule Hannover (A.K.); by the European Community Seventh Framework Programme contract ['CardioGeNet' 223463] (V.M.C.); and a National Institutes of Health grant from the National Institute of Neurological Disorders and Stroke (NINDS) [R01 NS039421] (D.J.E.). Deposited in PMC for release after 12 months.

Competing interests statement
The authors declare no competing financial interests.

Supplementary material
Supplementary material available online at
http://dev.biologists.org/lookup/suppl/doi:10.1242/dev.094524/-/DC1

References

Aanhaanen, W. T. J., Brons, J. F., Domínguez, J. N., Rana, M. S., Norden, J., Airik, R., Wakker, V., de Gier-de Vries, C., Brown, N. A., Kispert, A. et al. (2009). The Tbx2+ primary myocardium of the atrioventricular canal forms the atrioventricular node and the base of the left ventricle. *Circ. Res.* **104**, 1267-1274.

Ågren, M., Kogerman, P., Kleman, M. I., Wessling, M. and Toftgård, R. (2004). Expression of the PTCH1 tumor suppressor gene is regulated by alternative promoters and a single functional Gli-binding site. *Gene* **330**, 101-114.

Alvarez-Bolado, G., Rosenfeld, M. G. and Swanson, L. W. (1995). Model of forebrain regionalization based on spatiotemporal patterns of POU-III homeobox gene expression, birthdates, and morphological features. *J. Comp. Neurol.* **355**, 237-295.

Amar, A. P. and Weiss, M. H. (2003). Pituitary anatomy and physiology. *Neurosurg. Clin. N. Am.* **14**, 11-23, v.

Boogerd, C. J. J., Wong, L. Y. E., van den Boogaard, M., Bakker, M. L., Tessadori, F., Bakkers, J., 't Hoen, P. A. C., Moorman, A. F., Christoffels, V. M. and Barnett, P. (2011). Sox4 mediates Tbx3 transcriptional regulation of the gap junction protein Cx43. *Cell. Mol. Life Sci.* **68**, 3949-3961.

Brinkmeier, M. L., Potok, M. A., Davis, S. W. and Camper, S. A. (2007). TCF4 deficiency expands ventral diencephalon signaling and increases induction of pituitary progenitors. *Dev. Biol.* **311**, 396-407.

Brummelkamp, T. R., Kortlever, R. M., Lingbeek, M., Trettel, F., MacDonald, M. E., van Lohuizen, M. and Bernards, R. (2002). TBX-3, the gene mutated in Ulnar-Mammary Syndrome, is a negative regulator of p19ARF and inhibits senescence. *J. Biol. Chem.* **277**, 6567-6572.

Bussen, M., Petry, M., Schuster-Gossler, K., Leitges, M., Gossler, A. and Kispert, A. (2004). The T-box transcription factor Tbx18 maintains the separation of anterior and posterior somite compartments. *Genes Dev.* **18**, 1209-1221.

Daikoku, S., Chikamori, M., Adachi, T. and Maki, Y. (1982). Effect of the basal diencephalon on the development of Rathke's pouch in rats: a study in combined organ cultures. *Dev. Biol.* **90**, 198-202.

Dasen, J. S. and Rosenfeld, M. G. (2001). Signaling and transcriptional mechanisms in pituitary development. *Annu. Rev. Neurosci.* **24**, 327-355.

Dattani, M. T., Martinez-Barbera, J. P., Thomas, P. Q., Brickman, J. M., Gupta, R., Mårtensson, I. L., Toresson, H., Fox, M., Wales, J. K., Hindmarsh, P. C. et al. (1998). Mutations in the homeobox gene HESX1/Hesx1 associated with septo-optic dysplasia in human and mouse. *Nat. Genet.* **19**, 125-133.

De Moerlooze, L., Spencer-Dene, B., Revest, J. M., Hajihosseini, M., Rosewell, I. and Dickson, C. (2000). An important role for the IIIb isoform of fibroblast growth factor receptor 2 (FGFR2) in mesenchymal-epithelial signalling during mouse organogenesis. *Development* **127**, 483-492.

Echelard, Y., Epstein, D. J., St-Jacques, B., Shen, L., Mohler, J., McMahon, J. A. and McMahon, A. P. (1993). Sonic hedgehog, a member of a family of putative signaling molecules, is implicated in the regulation of CNS polarity. *Cell* **75**, 1417-1430.

Epstein, D. J., McMahon, A. P. and Joyner, A. L. (1999). Regionalization of Sonic hedgehog transcription along the anteroposterior axis of the mouse central nervous system is regulated by Hnf3-dependent and -independent mechanisms. *Development* **126**, 281-292.

Ericson, J., Norlin, S., Jessell, T. M. and Edlund, T. (1998). Integrated FGF and BMP signaling controls the progression of progenitor cell differentiation and the emergence of pattern in the embryonic anterior pituitary. *Development* **125**, 1005-1015.

Fulcoli, F. G., Huynh, T., Scambler, P. J. and Baldini, A. (2009). Tbx1 regulates the BMP-Smad1 pathway in a transcription independent manner. *PLoS ONE* **4**, e6049.

Furukawa, T., Kozak, C. A. and Cepko, C. L. (1997). rax, a novel paired-type homeobox gene, shows expression in the anterior neural fold and developing retina. *Proc. Natl. Acad. Sci. USA* **94**, 3088-3093.

Gaston-Massuet, C., Andoniadou, C. L., Signore, M., Sajedi, E., Bird, S., Turner, J. M. A. and Martinez-Barbera, J.-P. (2008). Genetic interaction between the homeobox transcription factors HESX1 and SIX3 is required for normal pituitary development. *Dev. Biol.* **324**, 322-333.

Habets, P. E. M. H., Moorman, A. F. M., Clout, D. E. W., van Roon, M. A., Lingbeek, M., van Lohuizen, M., Campione, M. and Christoffels, V. M. (2002). Cooperative action of Tbx2 and Nkx2.5 inhibits ANF expression in the atrioventricular canal: implications for cardiac chamber formation. *Genes Dev.* **16**, 1234-1246.

Hatakeyama, J., Bessho, Y., Katoh, K., Ookawara, S., Fujioka, M., Guillemot, F. and Kageyama, R. (2004). Hes genes regulate size, shape and histogenesis of the nervous system by control of the timing of neural stem cell differentiation. *Development* **131**, 5539-5550.

Hoogaars, W. M., Engel, A., Brons, J. F., Verkerk, A. O., de Lange, F. J., Wong, L. Y., Bakker, M. L., Clout, D. E., Wakker, V., Barnett, P. et al. (2007). Tbx3 controls the sinoatrial node gene program and imposes pacemaker function on the atria. *Genes Dev.* **21**, 1098-1112.

Ishibashi, M. and McMahon, A. P. (2002). A sonic hedgehog-dependent signaling relay regulates growth of diencephalic and mesencephalic primordia in the early mouse embryo. *Development* **129**, 4807-4819.

Jacobs, J. J., Keblusek, P., Robanus-Maandag, E., Kristel, P., Lingbeek, M., Nederlof, P. M., van Welsem, T., van de Vijver, M. J., Koh, E. Y., Daley, G. Q. et al. (2000). Senescence bypass screen identifies TBX2, which represses Cdkn2a (p19(ARF)) and is amplified in a subset of human breast cancers. *Nat. Genet.* **26**, 291-299.

Jean, D., Bernier, G. and Gruss, P. (1999). Six6 (Optx2) is a novel murine Six3-related homeobox gene that demarcates the presumptive pituitary/hypothalamic axis and the ventral optic stalk. *Mech. Dev.* **84**, 31-40.

Jeong, Y. and Epstein, D. J. (2003). Distinct regulators of Shh transcription in the floor plate and notochord indicate separate origins for these tissues in the mouse node. *Development* **130**, 3891-3902.

Jeong, Y., El-Jaick, K., Roessler, E., Muenke, M. and Epstein, D. J. (2006). A functional screen for sonic hedgehog regulatory elements across a 1 Mb interval identifies long-range ventral forebrain enhancers. *Development* **133**, 761-772.

Jeong, Y., Leskow, F. C., El-Jaick, K., Roessler, E., Muenke, M., Yocum, A., Dubourg, C., Li, X., Geng, X., Oliver, G. et al. (2008). Regulation of a remote Shh forebrain enhancer by the Six3 homeoprotein. *Nat. Genet.* **40**, 1348-1353.

Kelberman, D., Rizzoti, K., Avilion, A., Bitner-Glindzicz, M., Cianfarani, S., Collins, J., Chong, W. K., Kirk, J. M. W., Achermann, J. C., Ross, R. et al. (2006). Mutations within Sox2/SOX2 are associated with abnormalities in the

hypothalamo-pituitary-gonadal axis in mice and humans. *J. Clin. Invest.* **116**, 2442-2455.
Kenney, A. M., Cole, M. D. and Rowitch, D. H. (2003). Nmyc upregulation by sonic hedgehog signaling promotes proliferation in developing cerebellar granule neuron precursors. *Development* **130**, 15-28.
Kimura, S., Hara, Y., Pineau, T., Fernandez-Salguero, P., Fox, C. H., Ward, J. M. and Gonzalez, F. J. (1996). The T/ebp null mouse: thyroid-specific enhancer-binding protein is essential for the organogenesis of the thyroid, lung, ventral forebrain, and pituitary. *Genes Dev.* **10**, 60-69.
Kioussi, C., O'Connell, S., St-Onge, L., Treier, M., Gleiberman, A. S., Gruss, P. and Rosenfeld, M. G. (1999). Pax6 is essential for establishing ventral-dorsal cell boundaries in pituitary gland development. *Proc. Natl. Acad. Sci. USA* **96**, 14378-14382.
Kita, A., Imayoshi, I., Hojo, M., Kitagawa, M., Kokubu, H., Ohsawa, R., Ohtsuka, T., Kageyama, R. and Hashimoto, N. (2007). Hes1 and Hes5 control the progenitor pool, intermediate lobe specification, and posterior lobe formation in the pituitary development. *Mol. Endocrinol.* **21**, 1458-1466.
Kuhlbrodt, K., Herbarth, B., Sock, E., Hermans-Borgmeyer, I. and Wegner, M. (1998). Sox10, a novel transcriptional modulator in glial cells. *J. Neurosci.* **18**, 237-250.
Lingbeek, M. E., Jacobs, J. J. L. and van Lohuizen, M. (2002). The T-box repressors TBX2 and TBX3 specifically regulate the tumor suppressor gene p14ARF via a variant T-site in the initiator. *J. Biol. Chem.* **277**, 26120-26127.
Lu, J., Li, X.-P., Dong, Q., Kung, H.-F. and He, M.-L. (2010). TBX2 and TBX3: the special value for anticancer drug targets. *Biochim. Biophys. Acta* **1806**, 268-274.
Lüdtke, T. H. W., Christoffels, V. M., Petry, M. and Kispert, A. (2009). Tbx3 promotes liver bud expansion during mouse development by suppression of cholangiocyte differentiation. *Hepatology* **49**, 969-978.
Lüdtke, T. H. W., Farin, H. F., Rudat, C., Schuster-Gossler, K., Petry, M., Barnett, P., Christoffels, V. M. and Kispert, A. (2013). Tbx2 controls lung growth by direct repression of the cell cycle inhibitor genes Cdkn1a and Cdkn1b. *PLoS Genet.* **9**, e1003189.
Manning, L., Ohyama, K., Saeger, B., Hatano, O., Wilson, S. A., Logan, M. and Placzek, M. (2006). Regional morphogenesis in the hypothalamus: a BMP-Tbx2 pathway coordinates fate and proliferation through Shh downregulation. *Dev. Cell* **11**, 873-885.
Marcinkiewicz, M., Day, R., Seidah, N. G. and Chrétien, M. (1993). Ontogeny of the prohormone convertases PC1 and PC2 in the mouse hypophysis and their colocalization with corticotropin and alpha-melanotropin. *Proc. Natl. Acad. Sci. USA* **90**, 4922-4926.
Mathers, P. H., Grinberg, A., Mahon, K. A. and Jamrich, M. (1997). The Rx homeobox gene is essential for vertebrate eye development. *Nature* **387**, 603-607.
Medina-Martinez, O., Amaya-Manzanares, F., Liu, C., Mendoza, M., Shah, R., Zhang, L., Behringer, R. R., Mahon, K. A. and Jamrich, M. (2009). Cell-autonomous requirement for rx function in the mammalian retina and posterior pituitary. *PLoS ONE* **4**, e4513.
Mill, P., Mo, R., Hu, M. C., Dagnino, L., Rosenblum, N. D. and Hui, C.-C. (2005). Shh controls epithelial proliferation via independent pathways that converge on N-Myc. *Dev. Cell* **9**, 293-303.
Moorman, A. F., Houweling, A. C., de Boer, P. A. and Christoffels, V. M. (2001). Sensitive nonradioactive detection of mRNA in tissue sections: novel application of the whole-mount in situ hybridization protocol. *J. Histochem. Cytochem.* **49**, 1-8.
Morgan, S. M., Samulowitz, U., Darley, L., Simmons, D. L. and Vestweber, D. (1999). Biochemical characterization and molecular cloning of a novel endothelial-specific sialomucin. *Blood* **93**, 165-175.
Muzumdar, M. D., Tasic, B., Miyamichi, K., Li, L. and Luo, L. (2007). A global double-fluorescent Cre reporter mouse. *Genesis* **45**, 593-605.
Naiche, L. A., Harrelson, Z., Kelly, R. G. and Papaioannou, V. E. (2005). T-box genes in vertebrate development. *Annu. Rev. Genet.* **39**, 219-239.
Norlin, S., Nordström, U. and Edlund, T. (2000). Fibroblast growth factor signaling is required for the proliferation and patterning of progenitor cells in the developing anterior pituitary. *Mech. Dev.* **96**, 175-182.
Ohuchi, H., Hori, Y., Yamasaki, M., Harada, H., Sekine, K., Kato, S. and Itoh, N. (2000). FGF10 acts as a major ligand for FGF receptor 2 IIIb in mouse multi-organ development. *Biochem. Biophys. Res. Commun.* **277**, 643-649.
Oliver, G., Mailhos, A., Wehr, R., Copeland, N. G., Jenkins, N. A. and Gruss, P. (1995). Six3, a murine homologue of the sine oculis gene, demarcates the most anterior border of the developing neural plate and is expressed during eye development. *Development* **121**, 4045-4055.
Oppenheim, R. W., Homma, S., Marti, E., Prevette, D., Wang, S., Yaginuma, H. and McMahon, A. P. (1999). Modulation of early but not later stages of programmed cell death in embryonic avian spinal cord by sonic hedgehog. *Mol. Cell. Neurosci.* **13**, 348-361.
Plageman, T. F., Jr and Yutzey, K. E. (2005). T-box genes and heart development: putting the "T" in heart. *Dev. Dyn.* **232**, 11-20.
Pontecorvi, M., Goding, C. R., Richardson, W. D. and Kessaris, N. (2008). Expression of Tbx2 and Tbx3 in the developing hypothalamic-pituitary axis. *Gene Expr. Patterns* **8**, 411-417.
Potok, M. A., Cha, K. B., Hunt, A., Brinkmeier, M. L., Leitges, M., Kispert, A. and Camper, S. A. (2008). WNT signaling affects gene expression in the ventral diencephalon and pituitary gland growth. *Dev. Dyn.* **237**, 1006-1020.
Reményi, A., Lins, K., Nissen, L. J., Reinbold, R., Schöler, H. R. and Wilmanns, M. (2003). Crystal structure of a POU/HMG/DNA ternary complex suggests differential assembly of Oct4 and Sox2 on two enhancers. *Genes Dev.* **17**, 2048-2059.
Riccomagno, M. M., Martinu, L., Mulheisen, M., Wu, D. K. and Epstein, D. J. (2002). Specification of the mammalian cochlea is dependent on Sonic hedgehog. *Genes Dev.* **16**, 2365-2378.
Rizzoti, K., Brunelli, S., Carmignac, D., Thomas, P. Q., Robinson, I. C. and Lovell-Badge, R. (2004). SOX3 is required during the formation of the hypothalamo-pituitary axis. *Nat. Genet.* **36**, 247-255.
Scully, K. M. and Rosenfeld, M. G. (2002). Pituitary development: regulatory codes in mammalian organogenesis. *Science* **295**, 2231-2235.
Sheng, H. Z., Zhadanov, A. B., Mosinger, B., Jr, Fujii, T., Bertuzzi, S., Grinberg, A., Lee, E. J., Huang, S. P., Mahon, K. A. and Westphal, H. (1996). Specification of pituitary cell lineages by the LIM homeobox gene Lhx3. *Science* **272**, 1004-1007.
Simeone, A., Gulisano, M., Acampora, D., Stornaiuolo, A., Rambaldi, M. and Boncinelli, E. (1992). Two vertebrate homeobox genes related to the Drosophila empty spiracles gene are expressed in the embryonic cerebral cortex. *EMBO J.* **11**, 2541-2550.
Simeone, A., Acampora, D., Mallamaci, A., Stornaiuolo, A., D'Apice, M. R., Nigro, V. and Boncinelli, E. (1993). A vertebrate gene related to orthodenticle contains a homeodomain of the bicoid class and demarcates anterior neuroectoderm in the gastrulating mouse embryo. *EMBO J.* **12**, 2735-2747.
Singh, R., Horsthuis, T., Farin, H. F., Grieskamp, T., Norden, J., Petry, M., Wakker, V., Moorman, A. F. M., Christoffels, V. M. and Kispert, A. (2009). Tbx20 interacts with smads to confine tbx2 expression to the atrioventricular canal. *Circ. Res.* **105**, 442-452.
Sinha, S., Abraham, S., Gronostajski, R. M. and Campbell, C. E. (2000). Differential DNA binding and transcription modulation by three T-box proteins, T, TBX1 and TBX2. *Gene* **258**, 15-29.
Takuma, N., Sheng, H. Z., Furuta, Y., Ward, J. M., Sharma, K., Hogan, B. L., Pfaff, S. L., Westphal, H., Kimura, S. and Mahon, K. A. (1998). Formation of Rathke's pouch requires dual induction from the diencephalon. *Development* **125**, 4835-4840.
Treier, M., Gleiberman, A. S., O'Connell, S. M., Szeto, D. P., McMahon, J. A., McMahon, A. P. and Rosenfeld, M. G. (1998). Multistep signaling requirements for pituitary organogenesis in vivo. *Genes Dev.* **12**, 1691-1704.
Treier, M., O'Connell, S., Gleiberman, A., Price, J., Szeto, D. P., Burgess, R., Chuang, P. T., McMahon, A. P. and Rosenfeld, M. G. (2001). Hedgehog signaling is required for pituitary gland development. *Development* **128**, 377-386.
Vokes, S. A., Ji, H., McCuine, S., Tenzen, T., Giles, S., Zhong, S., Longabaugh, W. J. R., Davidson, E. H., Wong, W. H. and McMahon, A. P. (2007). Genomic characterization of Gli-activator targets in sonic hedgehog-mediated neural patterning. *Development* **134**, 1977-1989.
Wang, D., Yan, B., Rajapaksha, W. R. A. K. J. S. and Fisher, T. E. (2009). The expression of voltage-gated ca2+ channels in pituicytes and the up-regulation of L-type ca2+ channels during water deprivation. *J. Neuroendocrinol.* **21**, 858-866.
Wang, Y. Y., Martin, J. F. J. and Bai, C. B. C. (2010). Direct and indirect requirements of Shh/Gli signaling in early pituitary development. *Dev. Biol.* **348**, 199-209.
Watanabe, Y. G. (1982). Effects of brain and mesenchyme upon the cytogenesis of rat adenohypophysis in vitro. I. Differentiation of adrenocorticotropes. *Cell Tissue Res.* **227**, 257-266.
Zhang, L., Mathers, P. H. and Jamrich, M. (2000). Function of Rx, but not Pax6, is essential for the formation of retinal progenitor cells in mice. *Genesis* **28**, 135-142.
Zhao, Y., Morales, D. C., Hermesz, E., Lee, W.-K., Pfaff, S. L. and Westphal, H. (2006). Reduced expression of the LIM-homeobox gene Lhx3 impairs growth and differentiation of Rathke's pouch and increases cell apoptosis during mouse pituitary development. *Mech. Dev.* **123**, 605-613.
Zhao, L., Li, G. and Zhou, G.-Q. (2009). SOX9 directly binds CREB as a novel synergism with the PKA pathway in BMP-2-induced osteochondrogenic differentiation. *J. Bone Miner. Res.* **24**, 826-836.
Zhao, Y., Mailloux, C. M., Hermesz, E., Palkóvits, M. and Westphal, H. (2010). A role of the LIM-homeobox gene Lhx2 in the regulation of pituitary development. *Dev. Biol.* **337**, 313-323.
Zhao, L., Zevallos, S. E., Rizzoti, K., Jeong, Y., Lovell-Badge, R. and Epstein, D. J. (2012). Disruption of SoxB1-dependent Sonic hedgehog expression in the hypothalamus causes septo-optic dysplasia. *Dev. Cell* **22**, 585-596.
Zhu, X., Gleiberman, A. S. and Rosenfeld, M. G. (2007). Molecular physiology of pituitary development: signaling and transcriptional networks. *Physiol. Rev.* **87**, 933-963.